Microbial Cell Factories

RESEARCH

Open Access

Hyper-porous encapsulation of microbes for whole cell biocatalysis and biomanufacturing

Jingyi Zhang[1], Keziah Chang[1], Joyce Tay[1], Elaine Tiong[2], Elena Heng[2], Theresa Seah[1,3], Yi Wee Lim[4], Guangrong Peh[4], Yee Hwee Lim[4], Fong Tian Wong[2,4] and Cyrus W. Beh[1*]

Abstract

Biocatalysis using whole cell biotransformation presents an alternative approach to producing complex molecules when compared to traditional synthetic chemical processes. This method offers several advantages, including scalability, self-contained co-factor recycling systems, the use of cost-effective raw materials, and reduced purification costs. Notably, biotransformation using microbial consortia provides benefits over monocultures by enhancing biosynthesis efficiency and productivity through division of labor and a reduction in metabolic burden. However, reliably controlling microbial cell populations within a consortium remains a significant challenge. In this work, we address this challenge through mechanical constraints. We describe the encapsulation and immobilization of cells in a hyper-porous hydrogel block, using methods and materials that are designed to be amenable to industrial scale-up. The porosity of the block provides ample nutrient access to ensure good cell viability, while the mechanical properties of the hydrogel matrix were optimized for *Escherichia coli* encapsulation, effectively limiting their proliferation while sustaining recombinant protein production. We also demonstrated the potential of this method for achieving stable co-cultivation of microbes by maintaining two different microbial strains spatially in a single porous hydrogel block. Finally, we successfully applied encapsulation to enable biotransformation in a mixed culture. Unlike its non-encapsulated counterpart, encapsulated *E. coli* expressing RadH halogenase achieved halogenation of the genistein substrate in a co-culture with genistein-producing *Streptomyces*. Overall, our strategy of controlling microbial cell populations through physical constraints offers a promising approach for engineering synthetic microbial consortia for biotransformation at an industrial scale.

Keywords Cell immobilization, Microencapsulation, Co-culture, Biocatalysis

*Correspondence:
Cyrus W. Beh
beh_cyrus@bti.a-star.edu.sg
[1] Bioprocessing Technology Institute, Agency for Science, Technology and Research (A*STAR), 20 Biopolis Way, #06-01 Centros, Singapore 138668, Singapore
[2] Institute of Molecular and Cell Biology (IMCB), Agency for Science, Technology and Research (A*STAR), 61 Biopolis Drive, Proteos, #07-06, Singapore 138673, Singapore
[3] Department of Biomedical Engineering, National University of Singapore, 4 Engineering Drive 3, #04-08, Singapore 117583, Singapore
[4] Institute of Sustainability for Chemicals, Energy and Environment (ISCE2), Agency for Science, Technology and Research (A*STAR), 8 Biomedical Grove, Neuros, #07-01, Singapore 138665, Singapore

Introduction

Compared to traditional chemical processes, biocatalysis offer opportunities for environmentally friendly manufacturing of complex molecules. With its high stereochemical specificity and mild reaction conditions, biocatalysis often requires less chemicals, waste and energy [1, 2]. While industrial practice has tended to favor immobilized enzymes over whole cell biocatalysts in recent years [2], the latter still offers some advantages over cell-free enzymes [3]. For example, cell-free systems often require the use of purified enzymes, which increases the overall time and cost of production [3]. In many reactions, it is also necessary to supply expensive co-factors, or otherwise develop recycling systems, further increasing production costs [2]. On the contrary, whole-cell biocatalysts contain inherent co-factor recycling systems, simplifying the process. These cells can also convert cheap raw materials into high-value chemicals that have applications in pharmaceutical industry [3–5]. For these reasons, research into whole-cell biocatalysis have remained active [4–6].

These advantages notwithstanding, several challenges persist for the adoption of whole-cell biocatalyst. Traditionally, a single industrial strain is engineered to incorporate the entire synthetic pathway [7], though the heavy gene expression burden can result in reduced efficiency and robustness [8]. In nature, microbial consortia comprising different species accomplish the task of performing difficult chemical tasks by division of labour. Attributed to their collective metabolic abilities and synergistic interactions, a microbial consortium confers advantages such as robustness, reduced metabolic burden while exploiting unique catalytic ability of the individual species, enabling enhanced functional capabilities productivity [9]. Some groups have since designed co-cultivation systems, which allows for a reduction in metabolic load and ultimately leading to a more dynamic cell population, even in systems involving a mixture of prokaryotic and eukaryotic organisms [6, 7]. However, the challenge lies in achieving stable and efficient synthetic microbial consortia for biomanufacturing, where species artificially cultured together co-exists in equilibrium and each organism contributing to the overall functionality without dominance [10, 11]. This may involve elaborate strain engineering to create a mutualistic relationship between the consortia members [7].

To address these challenges, we hypothesize that encapsulating *Escherichia coli* cells in a hydrogel matrix with appropriate mechanical properties could help limit their proliferation. By restricting their growth, we can not only maintain ratios of bacterial populations within a mixed community but also promote efficient resource allocation and reduce metabolic stress by decoupling growth from production [12]. Prior studies have investigated the effects of physical constraints on bacterial growth and physiological activity. For instance, applying mechanical compression to *E. coli* alters their shape from a rod-like to a flattened geometry without significantly affecting their growth rate or protein synthesis, indicating the adaptive capability of bacteria under physical constraints [13]. In the context of hydrogel encapsulation, bacteria growth and metabolic activity can be modulated by tuning the viscoelastic properties of Pluronic F127 hydrogels through adjusting the degree of acrylate crosslink, emphasizing the impact of matrix stiffness on growth dynamics [14]. Furthermore, alginate core-shell confinement enables controlled bacterial colonization with high cell density, maintaining physiology and functionality over 10 days while preventing overgrowth [15]. Additionally, hollow-core polyelectrolyte-coated chitosan alginate microcapsules act as selectively permeable barriers allowing nutrient exchange while preventing cell escape, supporting high-density bacterial growth and sustained viability [16].

In this report, we developed an encapsulation strategy to achieve control of microbial cell populations by immobilizing cells in a hyper-porous hydrogel block. This permits ample access to nutrients by the cells, while allowing for media changes to be carried out. We showed that different microbial strains can be maintained in a single porous hydrogel block, demonstrating the potential of this method for achieving stable co-culture. Finally, we demonstrated that these immobilized *E. coli* retained their capabilities for recombinant protein expression and as whole cell biocatalysts.

Materials and methods

Materials

Gelatin from porcine skin (gel strength 300, type A) was purchased from Sigma Aldrich. Microbial transglutaminase (mTG) was purchased from Modernist Kitchen. Phosphate buffered saline (PBS) was purchased from Gibco. Collagenase from Clostridium histolyticum type IV was purchased from Merck. Hanks' Balanced Salt Solution (1X) (HBSS) and Nunc Lab-Tek chamber were purchased from Thermo Scientific. Mueller Hinton II Broth (MHB) was purchased from BD Biosciences. Organic solvents (DMSO, ethanol, acetone, acetonitrile) were purchased from Sigma Aldrich. 96-well clear flat bottom polystyrene TC-treated microplates were purchased from Corning. Petri dish (94 mm × 16 mm), not-treated, polystyrene was obtained from Greiner. Samples were imaged using Carl Zeiss LSM 700 confocal microscopy. Particles were prepared using handheld extruder equipped with a coarse 3 mm holes and mesh with pore size (diameter) of 340 μm. Biowave Co8000

cell density meter was used to measure the OD_{600} readings. BL21 (DE3) *E. coli* was obtained from ThermoFisher Scientific (Invitrogen) and plasmid for RadH expression was obtained from previous study [17]. *Streptomyces* sp. A1301, which was previously characterized in an earlier investigation, was used in this study [18].

mTG toxicity test with *E. coli* in MHB

MHB buffer (1.76% w/v) was prepared by dissolving MHB powder in MilliQ water. Using a stock solution of mTG in MHB buffer (20% w/v), eight different concentrations (0.07813%, 0.156%, 0.3125%, 0.625%, 1.25%, 2.5%, 5%, 10% w/v) were prepared via serial dilution. *E. coli* containing a plasmid for expression of enhanced green fluorescent protein (eGFP) was grown in Luria-Bertani (LB) with resistance at 37 °C and 200 rpm until it reached OD_{600} of 0.7. The *E. coli* stock was then diluted a further 20,000× in each concentration of mTG solution in addition to a control group (pure MHB) with antibiotics included, resulting in a starting cell concentration of 4.18 ± 0.14 Log_{10}(colony-forming units (CFU)/mL). In a 96-well clear-bottom microplate, 200 µL of this solution was added to each well (N = 6), and the plate was incubated at 37 °C with shaking at 100 rpm for 18 h. After incubation, all wells for each concentration were collected for plating. Cells from each concentration were serially diluted (10^{-5} to 10^{-8}), plated on LB agar plates with antibiotics, and incubated overnight at 37 °C. Colony counts were taken the next day, and the results were reported as Log_{10}(CFU/mL) values for each mTG concentration and the control group.

Preparation of hyper-porous hydrogel

20% w/v gelatin solution with 2.5% w/v mTG was prepared at 37°C and mixed thoroughly to achieve a homogeneous solution. After cooling, hydrogel was passed through the extruder multiple times to form microparticles. The microparticles were then rinsed with 5% w/v mTG solution before submerging in the mTG solution at room temperature overnight, resulting in the formation of a hyper-porous, granular block scaffolds. The scaffolds after overnight crosslinking are designated as "Day 0".

Granular blocks were washed in MilliQ water and shaken in individual flasks at 37 °C and 100 rpm. Each block was cultured in 20 mL LB with 5, 10, and 20% v/v organic solvent (DMSO, ethanol, acetone, acetonitrile) containing antibiotics and 0.1 mM Isopropyl ß-D-1-thiogalactopyranoside (IPTG). Controls of blocks cultured in 20 mL LB with antibiotics and 0.1 mM IPTG were conducted as well. Dimensions of the blocks (length, width and height) were taken daily with vernier callipers to calculate the volume.

Thermal stability and porosity analysis of hydrogel blocks

Hydrogel blocks were prepared using 10% w/v gelatin with 0.2% w/v mTG, 10% w/v gelatin with 2.5% w/v mTG, and 20% w/v gelatin with 2.5% w/v mTG. After overnight crosslinking, the hydrogel blocks were gently dabbed dry using Kimwipes to remove the PBS from the pores before conducting an initial porosity test, where blue dyed water was dripped onto the top of the hydrogel blocks. The hydrogel blocks were then soaked in PBS and subjected to accelerated melting at 75 °C for 10 min. Following thermal treatment, the blocks were dabbed dry again and re-evaluated for porosity using blue dyed water.

Encapsulation of *E. coli*

For *E. coli* encapsulation, gelatin and mTG solutions were prepared in LB broth containing IPTG and antibiotics. eGFP *E. coli* was seeded in LB with antibiotics and cultured at 37 °C and 220 rpm, followed by sub-culturing in 5 mL LB with antibiotics the next day to an OD_{600} of 0.4. Cells were then induced with 0.1 mM IPTG and left to incubate at 37 °C, 220 rpm for 1 h. Subsequently, the induced cells were added to the gelatin solution to achieve a final OD_{600} of 0.0023. The porous granular blocks were then prepared as described in "Preparation of hyper-porous hydrogel" section.

Release of cells from encapsulating hydrogel

Granular blocks were each rinsed with 100 mL MilliQ water to remove free bacteria. To release *E. coli* cells from the hydrogel, each granular block was shaken with 1 mL 0.5 mg/mL collagenase solution at 37 °C and 1500 rpm for 45 min. The collagenase solution was prepared by dissolving powdered collagenase in HBSS. The subsequent cell solution was neutralized with 2 mL LB and spun down at 3000 rpm for 10 min. The supernatant was discarded, and the cell pellet was resuspended in 5 mL LB. For CFU counts, cells were serially diluted to concentrations ranging from 10^{-6} to 10^{-11}, plated on LB agar plates with antibiotics and incubated at 37 °C overnight. Colony counts were taken the next day and results reported as Log_{10}(CFU/mL) values for each individual block.

Hydrogel stiffness experiments

10% w/v gelatin (with 2.5% w/v mTG) and 20% w/v gelatin (with 2.5% and 5% w/v mTG) solution were prepared by dissolving gelatin and mTG in PBS. Each resulting solution was allowed to crosslink at 37 °C for 1 h. After crosslinking, the gel was left to equilibrate to room temperature for an additional hour. A biopsy punch was used to create three disc-shaped samples per condition. Subsequently, compression tests were performed on these discs with varying crosslinking conditions (Instron 3340

frame). The stiffness (Young's modulus) was then calculated using the slope of the linear portion of the stress–strain curve obtained during the test.

Monitoring growth of encapsulated cells

Hydrogels of different stiffness containing eGFP-expressing *E. coli* are prepared as described, and cultured in LB media, 100 μg/mL ampicillin, and 0.1 mM IPTG. At predetermined time points, the hydrogels were retrieved from the culture flasks and rinsed with MilliQ water. Fluorescence and brightfield images were used to monitor the diameter of the colonies over time. Each condition contained 3 samples, with 20 colonies sized for each sample. Long term culture was performed using 20% w/v gelatin crosslinked with 2.5% w/v mTG. The samples were cultured as described in the previous paragraph, and colony size was monitored for 51 days.

Co-culture of microbial strains

Co-culture of *E. coli* containing eGFP- and DsRed-expressing plasmids was performed by preparing granules containing each microbial strain separately, and blending the granules together to form porous hydrogel blocks as previously described (Preparation of hyper-porous hydrogel section). The samples were then imaged after 48 h on the confocal microscope. The particle boundaries were determined using a combination of brightfield images and scattering by the hydrogel matrix.

Halogenation by encapsulated microbes

Streptomyces sp. A1301 was seeded for 3 days in SV2 media, followed by sub-culturing in 50 mL CA10LB [18] fermentation media. 3 mL culture was collected at 24 h for LCMS analysis before the addition of immobilized *E. coli* expressing RadH [17]. *E. coli* was seeded in LB with antibiotics and sub-cultured the next day in 20 mL LB with antibiotics until it reached OD_{600} of 0.4. Cells were induced with 0.1 mM IPTG and encapsulated before adding to the 24 h fermentation culture of *Streptomyces* sp. A1301. All samples were prepared in triplicates. Samples were taken at day 7 for analyses.

Results and discussions

Determining composition of hyperporous hydrogel blocks

Using a simple extrusion approach, we can routinely prepare hundreds of milliliters of gelatin microparticles in minutes, which can be laden with microbes by simply suspending the cells in the gelatin solution before gelation. Subsequent covalent crosslinking within the particles and at the particle-particle interfaces were performed using microbial transglutaminase (mTG) (Fig. 1A). After overnight crosslinking, covalent bonds between the particles are formed, resulting in a highly porous hydrogel block (Fig. 1B).

Since the typical microbial fermentation temperature is above the melting temperature of gelatin, incomplete covalent crosslinking can affect the porous architecture and overall stability of our hyperporous hydrogel blocks. To optimize the crosslinking conditions, gelatin was crosslinked with mTG, and the resulting hydrogel blocks were analyzed for thermal stability and porosity. The blocks were examined for porosity through the penetration of blue dyed water into the blocks before and after heating at 75 °C for 10 min. After thermal treatment, the hydrogel blocks with 2.5% w/v mTG retained their porosity, while we observed that the blue dyed solution remained on the surface of the hydrogel block at an mTG concentration of 0.2% w/v (Fig. 1C). We hypothesized that at 0.2% w/v, the hydrogel block had partially melted at higher temperatures, and upon cooling, the melted gelatin re-solidified in the interparticle spaces, reducing its porosity. Overall, these findings demonstrate that the higher mTG concentration promotes the formation of robust and porous hydrogel blocks, which is critical for maintaining the functional properties of the hydrogel over time (Fig. 1B).

The structural stability of the hydrogel construct in organic solvents (e.g. DMSO, ethanol, acetone, acetonitrile) [19] is an important consideration in encapsulation for biomanufacturing of small molecules, as it would enable biocatalytic processes at much higher substrate concentrations, achieving desired process intensification, and also promote longevity of the biocatalysts. Our preliminary results indicate that the hydrogel blocks are relatively stable in up to 20% organic solvents with only ~ 5% shrinkage after 6 days incubation (Supplementary Figure S1).

Our encapsulation uses readily available gelatin (a common byproduct of the meat industry) and mTG (an enzyme produced at industrial scale as a food additive), which permits adoption of our approach for industrial biomanufacturing without excessive cost. The ease of our preparation process is also more amenable to scaling up than bioprinting or gel bead formation approaches [6, 20]. The resulting hydrogel blocks are stable, and extremely porous, thus allowing media exchange to occur efficiently over long culture periods. Furthermore, since the cells will be encapsulated within gelatin microparticles just hundreds of microns in size, diffusion of nutrients and enzymatic substrates to the cells will be more efficient compared to bioprinted gels, which are typically millimeter-scale [6]. Our multi-pronged encapsulation strategy thus results in the formation of hydrogel blocks that can serve as immobilized, whole-cell biocatalysts (vide infra).

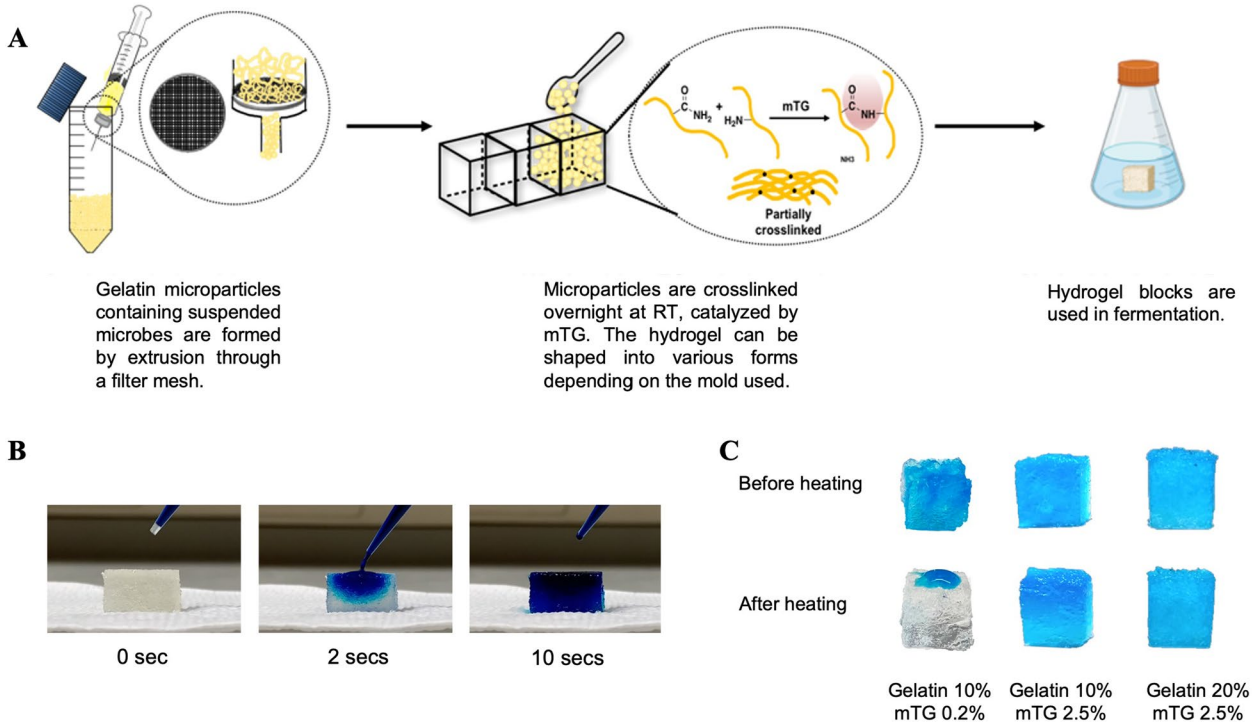

Fig. 1 **A** Preparation of porous hydrogels from microbe-laden hydrogel microparticles. **B** Permeability of hydrogel block with blue dyed water over 10 s. **C** Permeability of hydrogels with varying concentrations of mTG and gelatin. The 10% w/v gelatin hydrogel at 0.2% w/v mTG concentration loses its porous architecture after exposure to 75 °C for 10 min

Cell viability after crosslinking

Crosslinking of the hydrogel involves mTG, which can affect the viability of the *E. coli* due to its protein crosslinking ability [21–24]. To assess the biocompatibility of our process, we first studied the effects of exposure to different mTG concentrations on *E. coli* (Fig. 2A). The Log_{10}(CFU/mL) increased from 4.2 at the start of incubation to > 8.4 after 18 h. While there is a slight reduction in CFUs with increasing mTG concentration, this still corresponds to a 10^4- to 10^5-fold increase in CFUs across the tested mTG % range (Fig. 2A).

To further verify the viability of the cells after encapsulation, we compared the CFUs of the cells before and after encapsulation. For this measurement, cells were

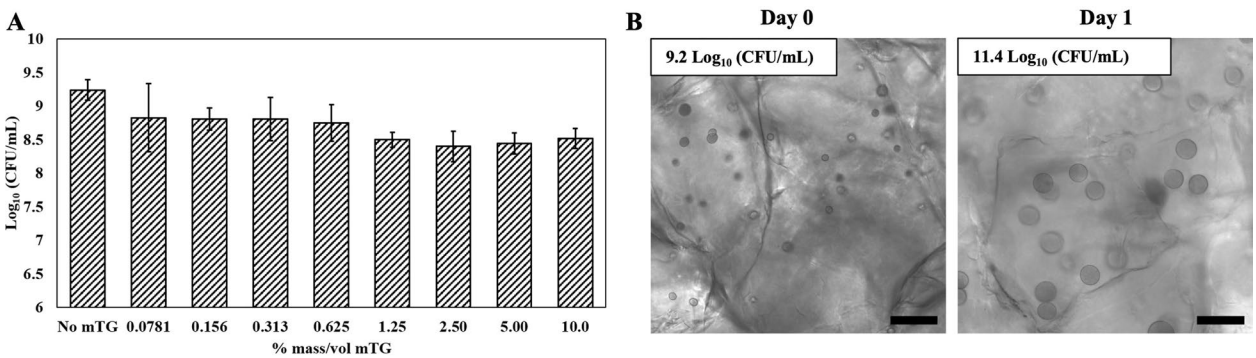

Fig. 2 Viability of cells after exposure to crosslinking conditions. **A** Cells were exposed to different concentrations of mTG in MHB media for 18 h (N = 6 per concentration). The Log_{10}(CFU/mL) value increased from 4.2 at the start of the experiment, to > 8.4 after incubation for all concentrations tested. **B** The cells encapsulated in gelatin microparticles form visible colonies, thus demonstrating their viability. Furthermore, the diameter of the colonies correlates with the Log_{10}(CFU/mL) value. Scale bar = 100 μm. The original, high-resolution version of Fig. 2B is provided in the Supplementary Figure S2

released by digesting the gelatin with collagenase. With an input of 5 Log_{10}(CFU/mL) before encapsulation, we achieved > 9 Log_{10}(CFU/mL) after overnight encapsulation (Fig. 2B, Day0)), and continued increasing thereafter (Fig. 2B, Day 1), thus proving that the cells are still viable.

The encapsulated cells are intended to serve as whole cell biocatalysts, which are advantageous over immobilized enzymes for their inherent co-factor recycling systems, and potential to convert cheap raw materials into high-value chemicals [3–5]. Since these functions can only be performed by living cells, it is thus important for the cells to remain viable after encapsulation, which we demonstrated with our results.

Achieving stable encapsulated cell population

Our approach uses physical means to constrain the growth of cells. We hypothesized that the material stiffness will affect the cell proliferation. To verify this, hydrogels containing *E. coli* with different stiffness were prepared by varying either/both gelatin and mTG concentrations. Samples were then imaged on a confocal microscope at fixed intervals to measure the colony sizes, which is correlated to cell numbers (Fig. 2B). Samples were also mechanically tested by compression to determine the Young's Modulus.

We found that the sample with the lowest stiffness (157 kPa) indeed resulted in the fastest cell growth (Fig. 3A), with the size of colonies increasing continuously. On the other hand, the colonies in the stiffer gels grew more slowly, and reached a plateau around Day 3. Using the 210 kPa gels, we encapsulated *E. coli* and cultured the hydrogel with daily LB media change over a prolonged period. The samples were retrieved for imaging at fixed intervals (n = 3, 20 colonies sized for each sample at each time point). We found that the cell growth was highest immediately post-encapsulation, and cell

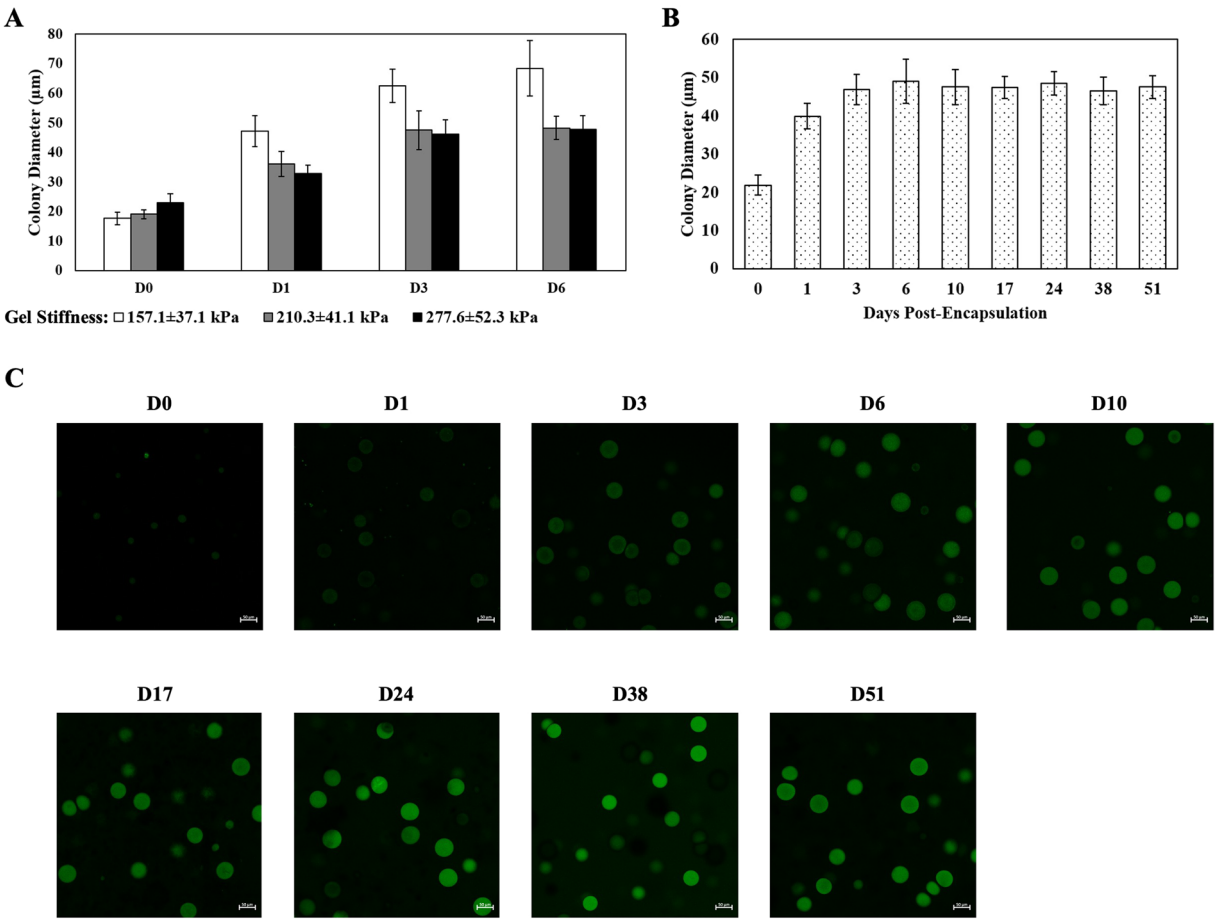

Fig. 3 Achieving stable *E. coli* cell numbers in hydrogel. **A** Hydrogels of different stiffness (157 kPa, 210 kPa, and 277 kPa) were prepared with *E. coli* encapsulated within. Colonies of cells in the 157 kPa gel (white bars) increased throughout the experiment, while the colony sizes in the stiffer gels stabilize around Day 3 (D3). D0 corresponds to the sample after overnight crosslinking. **B** Using the 210 kPa gels, we were able to achieve prolonged culture of cells, with colony sizes staying largely unchanged between D6 and D51. **C** We also observed almost no eGFP expression during the fastest colony growth from D0 to D3. eGFP expression gradually increased after D3 and continued up to D51

numbers stabilized from around Day 6 (Fig. 3B). On the other hand, eGFP signal was low initially but gradually increased from around Day 6 (Fig. 3C). At Day 51, eGFP signal can still be observed, concurring with previous reports that cells direct resources away from production during the growth phase [3, 25, 26].

Observations of constant colony diameters and consistent production of eGFP suggest that, as hypothesized, physical constraints imposed by our encapsulation strategy was able to limit growth, and in doing so, redirected resources from biomass production to recombinant protein production. This implication could significantly impact biotransformation efficiencies [12]. Furthermore, the steady state achieved by the encapsulation process can also simplify the determination of the optimal nutrient and substrate feed rate for the system.

Stable co-culture of *E. coli*

For multi-step biotransformation cascades, it may be advantageous to divide the synthetic pathway into multiple strains to reduce the workload. However, it is challenging to achieve stable ratios of strain populations for the duration of fermentation. In our initial experiments with non-immobilized culture fermentation, the ratios between strains were significantly inconsistent, ranging from 1:1 to 20:1 within 24 h (Supplementary Figure S3).

We then performed an immobilized co-culture of *E. coli* expressing either eGFP or DsRed by separately encapsulating each strain in gelatin microparticles, and crosslinking a blend of the two particle types into a single hydrogel block. This ensures that the two strains are compartmentalized in their respective particles. Confocal imaging further verified this approach, revealing clear boundaries within the hydrogel; each strain remained within its own particle, with no evidence of cross-ingression (Fig. 4).

This result illustrates how our approach can realize division of labor using multiple strains. By replacing the reporter genes with enzymes in an enzymatic cascade, cells responsible for different biocatalytic steps can be co-cultured without excessive competition. Moreover, achieving optimal efficiency in a multi-step process requires not just the presence of the cells/enzymes, but also matching the activity of each step. For whole-cell biocatalysts, this activity is determined in part by the cell numbers. Since encapsulated cell number reaches a plateau after some time (Achieving stable encapsulated cell population section), our approach may enable us to maintain specific cell ratios, even for cells that have significantly different growth rates.

More than a simple single-pot reaction, this configuration brings the two strains into close proximity, allowing efficient transport of substrates and intermediates between the strains, and can also result in high effective local concentration of various metabolites. This may be of particular interest to processes for which short-lived intermediates have to be quickly processed by downstream biotransformation reactions.

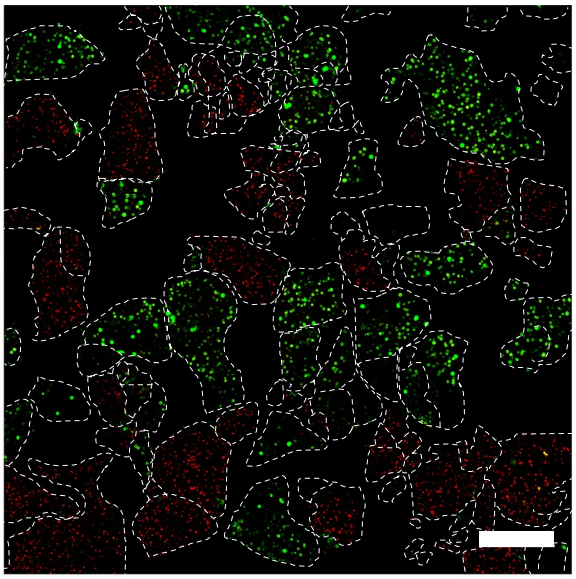

Fig. 4 Confocal image of co-culture of *E. coli* expressing eGFP (green) and DsRed (red) in a granular hydrogel block. White dashed lines demarcate each particle boundary. Encapsulated *E. coli* colonies remain compartmentalized to their own particles after 2 days of culture. Scale bar = 500 μm

Enzymatic halogenation reaction

To demonstrate the benefits of cell encapsulation in a co-culture biotransformation, we examined halogenation of genistein by RadH halogenase [17] heterologously expressed in immobilized *E. coli* in a co-culture fermentation with free *Streptomyces*. Here, we compared the extent of halogenation in the products with and without encapsulation (Fig. 5). As before, *E. coli* is encapsulated in our hyper-porous hydrogel block, and co-cultured with non-immobilized *Streptomyces*. Unlike the non-encapsulated system where only genistein (**1**) is detected, we observed production of chlorinated genistein products (**2** and **3**), as determined by LCMS-QTOF after 7 days of fermentation, for the encapsulated *E. coli* system (Fig. 5). These results indicate that diffusion of small molecule substrates and products through the hydrogel matrix is possible, and that the encapsulated microbes function as whole-cell biocatalysts more effectively than non-encapsulated form.

Currently, our experiment utilizes free *Streptomyces* in conjunction with encapsulated *E. coli* to showcase the benefits of an immobilized system. In future iterations,

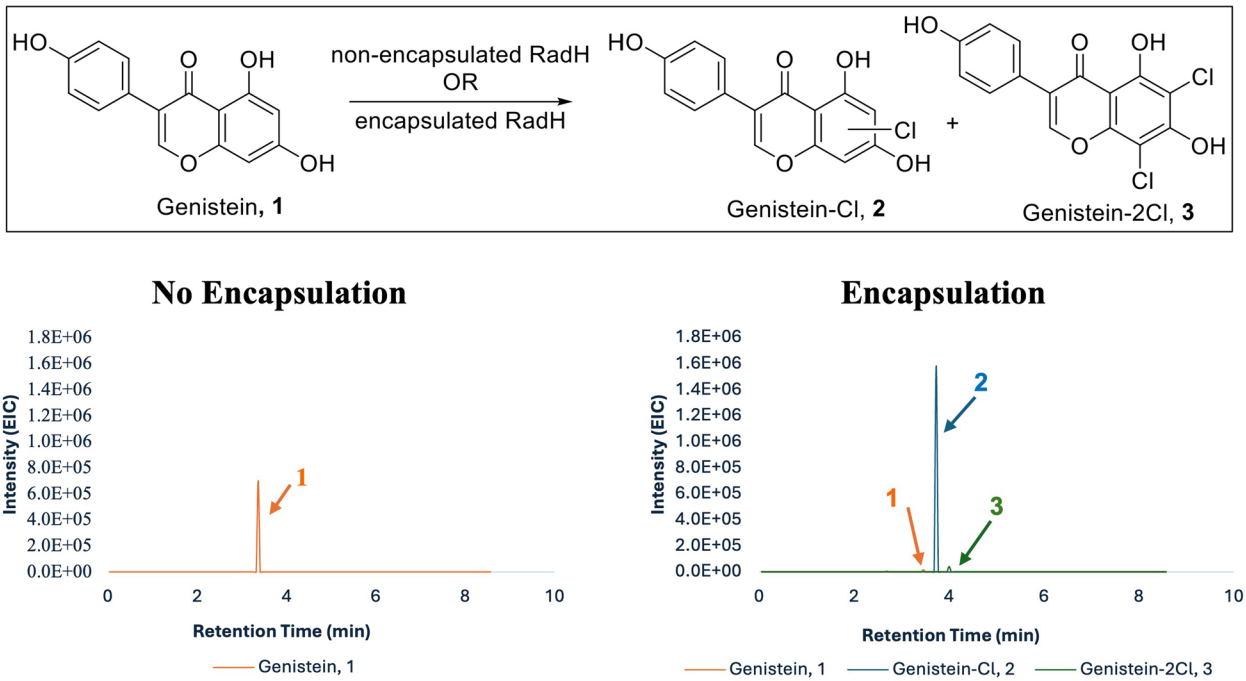

Fig. 5 Comparison of the chlorination of genistein (**1**) by encapsulated or free *E. coli* expressing RadH halogenases in a co-cultivation fermentation with free *Streptomyces* at day 7. Products were analyzed using LCMS-QTOF, with extracted ion chromatograms (EIC) highlighting the targeted masses of compounds **1**–**3**. Only EIC signals above 1.0E+04 are shown here

we envision further optimization through co-cultivation of different microbial populations encapsulated and immobilized within a single porous block, as shown in Fig. 4. Successful immobilization of microbes would in turn enable us to further engineer the process, including design of continuous flow reactors [27], optimization of the fermentation media, different feeding strategies [28], and mixed-phase extraction [29], all of which aim to facilitate continuous biomanufacturing with high efficiency.

Conclusions

In conclusion, these results demonstrate that our facile encapsulation method enables immobilization of functional whole-cell biocatalysts. The hyper-porous architecture allows easy access to nutrients in media and clearance of metabolites, thus ensuring long-term viability of the cells. It also facilitates transport of enzymatic substrates to the microbes, which remain enzymatically active after encapsulation, as evidenced by the successful halogenation of genistein. On the other hand, encapsulation physically limits cell proliferation, and allows the system to reach a steady state. This strategy can be used to facilitate stable co-culture of multiple biocatalysts, thereby opening up possibilities for efficient biotransformation cascades. While we have shown a proof-of-principle in this study, optimization of the various parameters is currently on-going to apply the approach to specific multi-step biotransformation, taking into account the activity of the enzymes, types of microbial cells used, expression levels in cells, and the optimal biocatalyst ratios. Looking forward, this approach could be used to create reactor modules that can efficiently perform complex biotransformation reactions, and that will fully realize the potential of our method in enhancing biocatalytic productivity.

Supplementary Information

The online version contains supplementary material available at https://doi.org/10.1186/s12934-025-02675-3.

Supplementary material 1.

Author contributions

C.W.B.: Conceptualization, methodology, software, data curation, formation analysis, visualization, writing—original draft-writing, writing—review and editing. J.Z., K.C., J.T.: Investigation, formal analysis, writing—original draft. T.S.: Investigation, formal analysis. F.T.W.: Conceptualization, investigation, methodology, writing—original draft-writing, writing—review and editing. G.P., E.T., E.H., Y.W.L.: Investigation, methodology, formal analysis. Y.H.L.; Conceptualization, Data analysis, writing—review and editing.

Funding

The authors gratefully acknowledge funding support from the Singapore Food Story (SFS) programme (W23W2D0009), Manufacturing Trade and Connectivity (MTC) Individual Research Grant (IRG) (M22K2c0086) and A*STAR Graduate Academy (to K.C. and T.S.).

Data availability
All data generated or analysed during this study are included in this published article [and its supplementary information files].

Declarations

Ethics approval and consent to participate
This article does not contain any studies involving human or animal subjects conducted by the authors.

Consent for publication
All authors approve this manuscript for publication.

Competing interests
The authors declare no competing interests.

Received: 19 December 2024 Accepted: 10 February 2025
Published online: 24 February 2025

References

1. Lee SY, Kim HU, Chae TU, Cho JS, Kim JW, Shin JH, Kim DI, Ko Y-S, Jang WD, Jang Y-S. A comprehensive metabolic engineering approach for the production of bio-based chemicals. Nat Catal. 2019;2:18–33.
2. France SP, Lewis RD, Martinez CA. The evolving nature of biocatalysis in pharmaceutical research and development. JACS Au. 2023;3:715–35.
3. Lin B, Tao Y. Whole-cell biocatalysts by design. Microbial Cell Factor. 2017;16:1–12.
4. Mähler C, Burger C, Kratzl F, Weuster-Botz D, Castiglione K. Asymmetric whole-cell bio-reductions of (r)-carvone using optimized ene reductases. Molecules. 2019;24:2550.
5. Nguyen HK, Minato T, Moniruzzaman M, Kiyasu Y, Ogo S, Yoon K-S. Selective formate production from h_2 and co_2 using encapsulated whole-cells under mild reaction conditions. J Biosci Bioeng. 2023;136:182–9.
6. Johnston TG, Yuan SF, Wagner JM, Yi X, Saha A, Smith P, Nelson A, Alper HS. Compartmentalized microbes and co-cultures in hydrogels for on-demand bioproduction and preservation. Nat Commun. 2020;11:563.
7. Zhou K, Qiao K, Edgar S, Stephanopoulos G. Distributing a metabolic pathway among a microbial consortium enhances production of natural products. Nat Biotechnol. 2015;33:377–83.
8. Xu P, Marsafari M, Zha J, Koffas M. Microbial coculture for flavonoid synthesis. Trends Biotechnol. 2020;38:686–8.
9. McCarty NS, Ledesma-Amaro R. Synthetic biology tools to engineer microbial communities for biotechnology. Trends Biotechnol. 2019;37(2):181–97.
10. Xu C, Yu H. Insights into constructing a stable and efficient microbial consortium. Chin J Chem Eng. 2021;30:112–20.
11. Roell GW, Zha J, Carr RR. Engineering microbial consortia by division of labor. Microbial Cell Factor. 2019;18:35.
12. Banerjee D, Mukhopadhyay A. Perspectives in growth production trade-off in microbial bioproduction. RSC Sustain. 2023;1(2):224–33.
13. Si F, Li B, Margolin W. Bacterial growth and form under mechanical compression. Sci Rep. 2015;5:11367.
14. Bhusari S, Sankaran S, delCampo A. Regulating bacterial behavior within hydrogels of tunable viscoelasticity. Adv Sci. 2022;9:2106026.
15. Jeong Y, Kong W, Lu T, Irudayaraj J. Soft hydrogel-shell confinement systems as bacteria-based bioactuators and biosensors. Biosens Bioelectron. 2023;219: 114809.
16. Girolamo SD, Puorger C, Lipps G. Stable and selective permeable hydrogel microcapsules for high-throughput cell cultivation and enzymatic analysis. Microbial Cell Fact. 2020;19:170.
17. Peh G, Gunawan GA, Tay T, Tiong E, Tan LL, Jiang S, Goh YL, Ye S, Wong J, Brown CJ. Further characterization of fungal halogenase radh and its homologs. Biomolecules. 2023;13:1081.
18. Tay DW, Tan LL, Heng E, Zulkarnain N, Ching KC, Wibowo M, Chin EJ, Tan ZYQ, Leong CY, Ng VWP. Exploring a general multi-pronged activation strategy for natural product discovery in actinomycetes. Commun Biol. 2024;7:50.
19. Gao L, Feng L, Sauer DF, Wittwer M, Hu Y, Schiffels J, Li X. Engineered living hydrogels for robust biocatalysis in pure organic solvents. Cell Rep Phys Sci. 2022. https://doi.org/10.1016/j.xcrp.2022.101054.
20. Jeong Y, Irudayaraj J. Multi-layered alginate hydrogel structures and bacteria encapsulation. Chem Commun. 2022;58(61):8584–7.
21. Kawai M, Takehana S, Takagi H. High-level expression of the chemically synthesized gene for microbial transglutaminase from streptoverticillium in *Escherichia coli*. Biosci Biotechnol Biochem. 1997;61:830–5.
22. Marx CK, Hertel TC, Pietzsch M. Soluble expression of a pro-transglutaminase from streptomyces mobaraensis in *Escherichia coli*. Enzyme Microbial Technol. 2007;40:1543–50.
23. Rickert M, Strop P, Lui V, Melton-Witt J, Farias SE, Foletti D, Shelton D, Pons J, Rajpal A. Production of soluble and active microbial transglutaminase in *Escherichia coli* for site-specific antibody drug conjugation. Protein Sci. 2016;25:442–55.
24. Yokoyama K-I, Nakamura N, Seguro K, Kubota K. Overproduction of microbial transglutaminase in *Escherichia coli*, in vitro refolding, and characterization of the refolded form. Biosci Biotechnol Biochem. 2000;64:1263–70.
25. Schrewe M, Julsing MK, Bühler B, Schmid A. Whole-cell biocatalysis for selective and productive c–o functional group introduction and modification. Chem Soc Rev. 2013;42:6346–77.
26. Carvalho CC. Whole cell biocatalysts: essential workers from nature to the industry. Microbial Biotechnol. 2017;10:250–63.
27. Zhang Z, Gao L, Boes A, Bajer B, Stotz J, Apitius L, Jakob F, Schneider ES, Sperling E, Held M, Emmler T, Schwaneberg U, Abetz V. An enzymatic continuous-flow reactor based on a pore-size matching nano- and isoporous block copolymer membrane. Nat Commun. 2024;15(1):3308.
28. Kopp J, Kittler S, Slouka C, Herwig C, Spadiut O, Wurm DJ. Repetitive fed-batch: a promising process mode for biomanufacturing with *E. coli*. Front Bioeng Biotechnol. 2020. https://doi.org/10.3389/fbioe.2020.573607.
29. Chaichola P, Weeranoppanant N. Advances in in situ and in-line liquid–liquid extraction for bioprocess intensification. React Chem Eng. 2023;8:2387–402.

Publisher's Note